

# **BOND CHARACTERISTICS OF VARIOUS FRP STRENGTHENING TECHNIQUES**

S. H. RIZKALLA

*Distinguished Professor, Department of Civil Engineering, North Carolina State  
University Campus Box 7533, Raleigh, NC, USA 27695-7533*

T. HASSAN

*Assistant Professor, Department of Civil Engineering, Ain-Shams University,  
Cairo, Egypt*

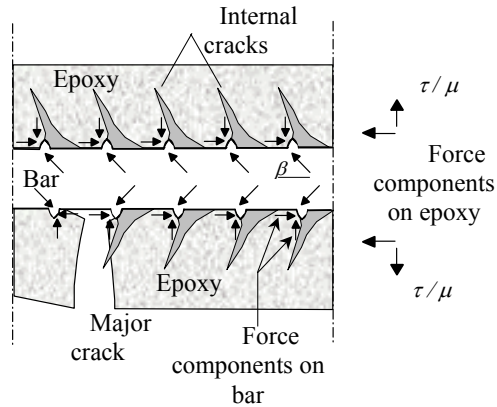
Strengthening of reinforced concrete structures using FRP has emerged as a potential solution to the problems associated with civil infrastructure. Many researchers have reported significant increases in strength and stiffness of concrete structures strengthened with FRP. Nevertheless, possible brittle failures of the strengthened system due to delamination of the FRP strips and/or sheets could limit the use of the full efficiency of the FRP system. This paper presents a bond failure hypothesis for near surface mounted FRP bars. Closed-form analytical solutions are proposed to predict the interfacial stresses for near surface mounted FRP strips and externally bonded FRP sheets. The models are calibrated by comparing the predicted behavior to test results. Quantitative criteria governing interfacial debonding failure of near surface mounted FRP bars, strips and externally bonded FRP sheets are established.

## **NSM FRP BARS**

Transfer of stresses from a deformed NSM FRP rod to the concrete is mainly by mechanical interlocking of the lugs with the surrounding epoxy. The resultant force exerted by the lug on the epoxy is inclined at an angle  $\beta$  to the axis of the bar as shown in Figure 1, where  $1/\tan \beta$  is the coefficient of friction,  $\mu$  between the bar and the adhesive. The radial component of the resultant force creates zones of high tensile stresses at the FRP-epoxy interface as well as at the concrete-epoxy interface. Finite element analysis was employed to provide in-depth understanding of the load transfer mechanism between NSM FRP bars and concrete. Figure 2 shows the mesh dimensions used in modelling a portion of a concrete beam strengthened with a NSM FRP bar. Groove dimensions, bar location and properties of

concrete and epoxy were set identical to the bond specimens tested by Rizkalla and Hassan, 2002<sup>1</sup>.

Figure 1. Forces between a NSM FRP bar and adhesive



Radial pressure was applied at the bar location to simulate the bond stresses transferred from the bar to the surrounding epoxy. Typical principal stresses transferred from the bar to the surrounding epoxy. Typical principal tensile stress distribution is shown in Figure 3. It should be noted that the elastic modulus of the adhesive is generally less than that of the concrete. Such a phenomenon results in a stress discontinuity at the concrete-epoxy interface as shown in Figure 3.

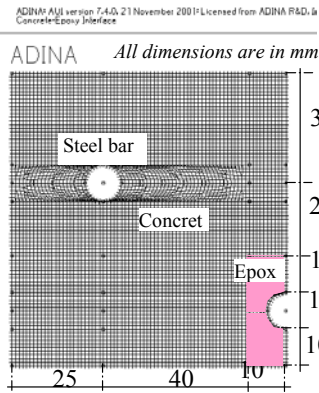


Figure 2. Mesh dimension for a portion of a concrete beam strengthened with a NSM FRP bar

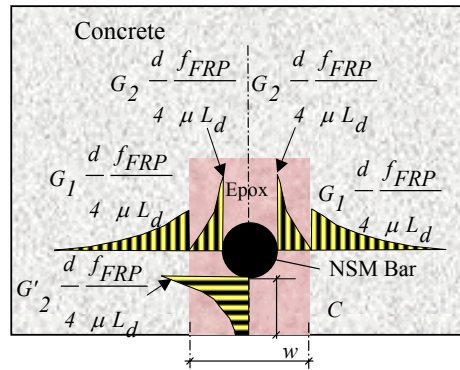


Figure 3. Typical tensile stress distribution around NSM FRP bars

High tensile stresses are observed at the concrete-epoxy interface as well as at the FRP-epoxy interface. Two different types of debonding failures could occur for NSM FRP bars. The first mode of failure is due to splitting of the epoxy cover as a result of high tensile stresses at the FRP-epoxy interface, and is termed “epoxy split failure”. Increasing the thickness of the epoxy

cover reduces the induced tensile stresses significantly. Furthermore, using adhesives of high tensile strength delays epoxy split failure. This type of debonding failure forms with longitudinal cracking through the epoxy cover. The second mode of failure is due to cracking of the concrete surrounding the epoxy adhesive and is termed “concrete split failure”. This mode of failure will take place when the tensile stresses at the concrete-epoxy interface reach the tensile strength of the concrete. Widening the groove minimizes the induced tensile stresses at the concrete-epoxy interface and increases the debonding loads of NSM bars. Concrete split failure was the governing mode of failure for the bond specimens tested by the authors<sup>1</sup>. Large epoxy cover and high tensile strength of the epoxy adhesive provided high resistance to epoxy split failure and shifted the failure to occur at the concrete-epoxy interface. The tangential bond stress,  $\tau$ , can be expressed as:

$$\tau = \frac{d}{4} \frac{f_{FRP}}{L_d} \quad (1)$$

where  $d$  is the diameter of the bar, and  $L_d$  is the embedment length needed to develop a stress of  $f_{FRP}$  in the NSM bar. If the coefficient of friction between the bar and the epoxy is  $\mu$ , the radial stresses,  $\sigma_{radial}$ , can be expressed as:

$$\sigma_{radial} = \frac{\tau}{\mu} = \frac{d}{4} \frac{f_{FRP}}{\mu L_d} \quad (2)$$

The tensile stresses at the concrete-epoxy interface,  $\sigma_{con-epoxy}$ , and at the FRP-epoxy interface,  $\sigma_{FRP-epoxy}$ , can be expressed in terms of the radial stress as follows:

$$\sigma_{con-epoxy} = G_1 \frac{d}{4} \frac{f_{FRP}}{\mu L_d} \quad (3)$$

$$\sigma_{FRP-epoxy} = G_2 \text{ or } G'_2 \left[ \frac{d}{4} \frac{f_{FRP}}{\mu L_d} \right] \quad (4)$$

where  $G_1$ ,  $G_2$  and  $G'_2$  are coefficients determined from the finite element analysis based on a unit radial pressure applied at the bar location and using specified groove dimensions, concrete and adhesive properties. The maximum tensile stress at the FRP-epoxy interface,  $\sigma_{FRP-epoxy}$ , depends on the coefficients  $G_2$  and  $G'_2$ , whichever is greater as shown in Figure 3. Equating the tensile strength of concrete to Eq. (3), the minimum

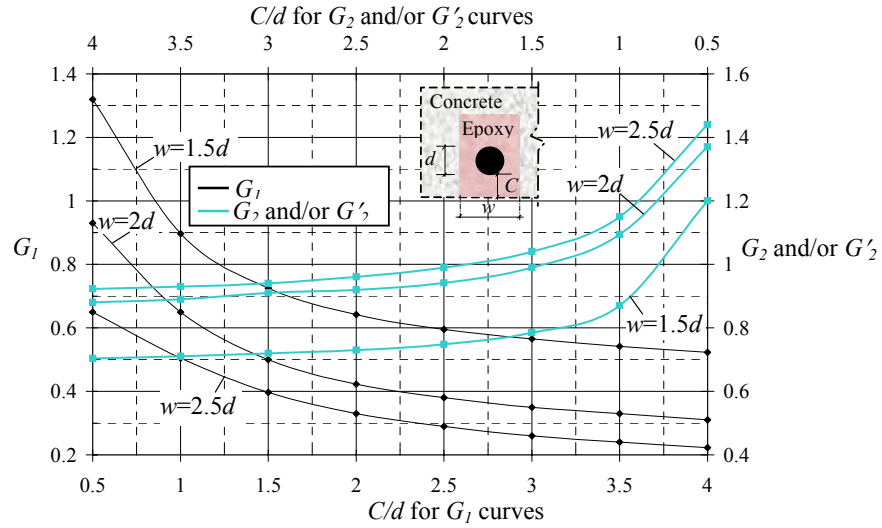
embedment length needed for NSM FRP bars to prevent concrete split failure can be expressed as:

$$L_d = G_1 \frac{d f_{FRP}}{4 \mu f_{ct}} \quad (5)$$

Equating the tensile strength of the adhesive to Eq. (4), the minimum embedment length needed for NSM FRP bars to avoid epoxy split failure shall not be less than:

$$L_d = G_2 \text{ or } G'_2 \left[ \frac{d f_{FRP}}{4 \mu f_{epoxy}} \right] \quad (6)$$

where  $f_{ct}$  and  $f_{epoxy}$  are the tensile strength of concrete and epoxy, respectively. Increasing the ratio of the elastic modulus of the concrete to that of the adhesive generates high tensile stresses at the concrete-epoxy interface and low tensile stresses at the FRP-epoxy interface. Practical values of the modular ratio could vary between 5 and 40. This range covers various types of concrete and adhesives that are commonly used in concrete structures. Figure 4 shows the proposed design chart for the development length of NSM FRP bars.



To simulate the design conditions for design purposes, NSM FRP bars  $G_1$  was evaluated for a modular ratio of 40. The coefficients,  $G_2$  and  $G'_2$  were evaluated for a modular ratio 5 and the greater value was plotted in Figure 4. The chart covers a wide range of possible epoxy covers and

accounts for three different groove sizes. Using the proposed design chart, the coefficients  $G_1$  and the greater value of either  $G_2$  or  $G'_2$  could be evaluated for a given groove width,  $w$ , and using a specified clear cover to bar diameter ratio ( $C/d$ ). The governing development length for NSM FRP bars could be predicted using the greater of Eqs. (5) and (6). The proposed approach compared very well with the test results and overestimated the development length of NSM CFRP bars by less than 5 percent<sup>1</sup>.

### NSM FRP STRIPS

This section presents a closed-form analytical solution to predict the interfacial shear stresses for NSM FRP strips. The model is validated by comparing the predicted values with test results<sup>2</sup>. The proposed model is based on the combined shear-bending model for externally bonded FRP plates and is given in Figure 5.

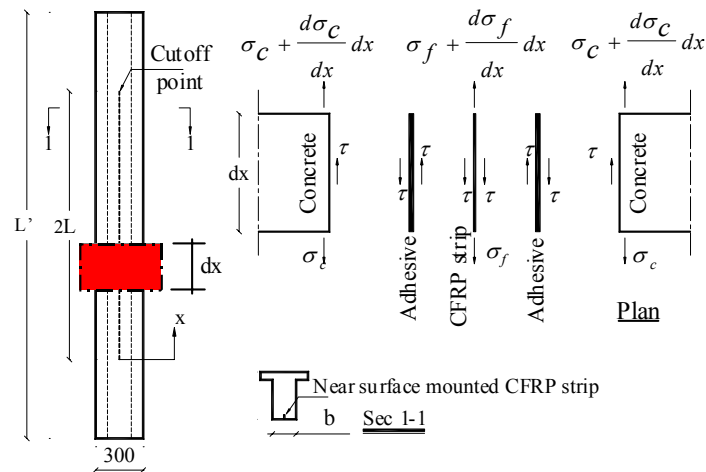


Figure 5. Analytical model for NSM FRP strips

The model is modified to account for the double bonded area of NSM strips. The model accounts also for the continuous reduction in flexural stiffness due to cracking of the concrete. Debonding of NSM strips is assumed to occur as a result of high shear stress concentration at cutoff point. The derivation of the model is reported elsewhere<sup>2</sup>. For simply supported beams subjected to a concentrated load,  $P$ , at midspan, the shear stress at the strip cutoff point,  $\tau$  can be expressed in terms of the effective moment of inertia,  $I_{eff}$ , and the thickness of the CFRP strip,  $t_f$ , as follows:

$$\tau = \frac{t_f}{2} \left[ \frac{nPl_o y}{2I_{eff}} \omega + \frac{nPy}{2I_{eff}} \right] \quad (7)$$

where,  $\omega^2 = \frac{2G_a}{t_a t_f E_f}$ ;  $n = \frac{E_f}{E_c}$ ;  $E_f$  is elastic modulus of the FRP strip,  $E_c$

is elastic modulus of concrete,  $G_a$  is the shear modulus of the adhesive,  $t_a$  is the thickness of the adhesive,  $l_o$  is the unbonded length of the strip;  $y$  is the distance from the strip to the neutral axis of the transformed section and  $I_{eff}$  is the effective moment of inertia of the transformed section. Debonding will occur when the shear stress reaches a maximum value, which depends on the concrete properties. Premature debonding of NSM CFRP strips is governed by the shear strength of the concrete. Other components of the system such as the adhesive and the CFRP strips have superior strength and adhesion properties compared to concrete. Knowing the compressive and tensile strength of concrete, the Mohr-Coulomb line, which is tangential to both Mohr's circles for pure tension and pure compression, can be represented and the maximum critical shear stress for the pure shear circle can be expressed as:

$$\tau_{\max} = \frac{f'_c f_{ct}}{f'_c + f_{ct}} \quad (8)$$

where  $f'_c$  is the compressive strength of concrete after 28 days and  $f_{ct}$  is the splitting tensile strength of concrete. Equating the shear strength proposed in Eq. (8) to the shear stress given in Eq. (7), debonding loads for NSM CFRP strips can be determined for simply supported beams subjected to a concentrated load at midspan. The development length is highly dependent on the dimensions of the strips, concrete properties, adhesive properties, internal steel reinforcement ratio, reinforcement configuration, type of loading, and groove width. The proposed model in Eqs. (7) and (8), can be used to estimate the development length of NSM strips of any configuration as follows:

a) Use the proposed Eqs. (7) and (8) to determine the debonding load of the strip for different embedment lengths as shown in Figure 6. The resulting curve represents a failure envelope due to debonding of the strip at cutoff point.

- b) Use a cracked section analysis at sections of maximum induced normal stresses and determine the ultimate load required to rupture the strip as shown in Figure 6.
- c) Determine the development length at the intersection of the line corresponding to flexural failure of the strip with the curve representing debonding failure at cutoff point. The calculated development length will preclude brittle failure due to debonding of the strips and will ensure full composite action between the strip and concrete up to failure. The proposed approach compared very well with the experimental results. The predicted debonding loads underestimated the measured values by less than 6%<sup>2</sup>.

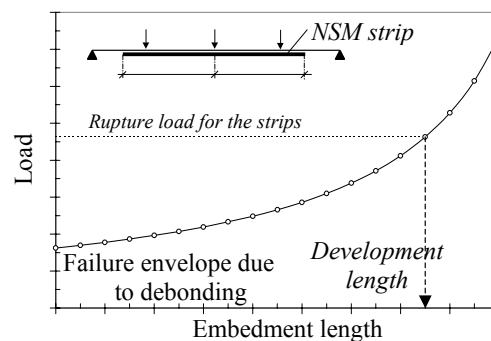


Figure 6. General procedures to determine the development length of NSM strips

## EXTERNALLY BONDED FRP SHEETS

The proposed approach modifies the analytical model developed by Malek et al., 1998<sup>3</sup>. New expressions for the moment of inertia and the neutral axis depth of the concrete section at cutoff points are introduced. An effective moment of inertia,  $I_{eff}$  and an effective neutral axis depth,  $y_{eff}$  are proposed to account for the continuous degradation in stiffness as cracking progresses. Both expressions were originally developed to predict the deflections of concrete members after cracking<sup>4</sup>. For simply supported beams subjected to a concentrated load at mid-span, the shear stress,  $\tau$ , and the normal stress,  $\sigma_n$ , at the ends of the externally bonded FRP reinforcement can be expressed by:

$$\tau = t_f \left[ \frac{nPl_o y_{eff}}{2I_{eff}} \omega' + \frac{nPy_{eff}}{2I_{eff}} \right] \quad (9)$$

$$\sigma_n = \frac{k_n}{2\beta^3} \left( \frac{V_f}{E_f I_f} - \frac{V_c + \beta M_a}{E_c I_{eff}} \right) \quad (10)$$

where  $V_c = V_o - b_f y_{eff} t_f \left( \frac{nPl_o y_{eff}}{2I_{eff}} \omega' + \frac{nPy_{eff}}{2I_{eff}} \right)$ ;  $\omega'^2 = \frac{G_a}{t_a t_f E_f}$ ;

$$k_n = \frac{E_a}{t_a}; V_f = -\frac{1}{2} b_f t_f^2 \left( \frac{nPl_o y_{eff}}{2I_{eff}} \omega' + \frac{nPy_{eff}}{2I_{eff}} \right); \beta = \left( \frac{k_n b_f}{4E_f I_f} \right)^{0.25}$$

and  $t_f$  is the thickness of the FRP sheets;  $t_a$  is the thickness of the adhesive;  $n$  is ratio of the elastic modulus of the FRP to that of the concrete;  $P$  is the applied concentrated load;  $l_o$  is the unbonded length of the FRP sheets;  $y_{eff}$  is the effective distance from the sheet to the neutral axis of the section;  $I_{eff}$  is the effective moment of inertia of the transformed section;  $I_f$  is the moment of inertia of the FRP sheets;  $E_a$ ,  $E_c$ ,  $E_f$  and are the modulus of elasticity of the adhesive, concrete and FRP, respectively;  $G_a$  is the shear modulus of the adhesive;  $b_f$  is the width of the FRP reinforcement;  $M_a$  is the applied moment on the concrete section at cutoff points; and  $V_o$  is the shear force in the concrete beam at the sheet cutoff point. Delamination of externally bonded FRP reinforcement can be determined using a critical combination of both normal and shear stresses at cutoff points. The critical combination of these two stresses was established by using a delamination circle<sup>5</sup>. The delamination circle provides a relationship between the shear strength,  $\tau_{max}$ , and the normal strength,  $\sigma_{nmax}$ . This relationship can be expressed in terms of the concrete compressive strength,  $f'_c$  and the concrete tensile strength,  $f_{ct}$  as follows:

$$\tau_{\max}^2 = \left( \frac{f'_c f_{ct}}{f'_c + f_{ct}} \right)^2 - \frac{f'_c f_{ct}}{(f'_c + f_{ct})^2} (f'_c - f_{ct}) \sigma_{n \max} - \frac{f'_c f_{ct}}{(f'_c + f_{ct})^2} \sigma_{n \max}^2 \quad (11)$$

The maximum normal and shear stresses are evaluated for the bond specimens tested by the authors using the proposed approach<sup>4</sup>. Interfacial debonding loads are predicted using Mohr-Coulomb failure criterion. The analysis is extended further to include specimens F1, C2 and G1 as well as specimens S1.0, S1.2 and S1.4 tested by other researchers to examine the validity of the proposed approach<sup>5,6</sup>. All the selected specimens experienced concrete cracking with various intensities at the sheets' cutoff points prior to delamination. Figure 7 shows the predicted delamination loads using the proposed approach compared with the experimental results. The predicted delamination loads using Malek's model, as well as those predicted using Brosens model, are also shown for comparison. The figure clearly indicates that delamination loads can be predicted with a sufficient accuracy using the proposed approach. Assuming uncracked concrete sections at the sheets' cutoff points overestimated the strength of the beams considerably and led to huge errors. Furthermore, using fully cracked concrete sections at cutoff points provided very conservative delamination loads.

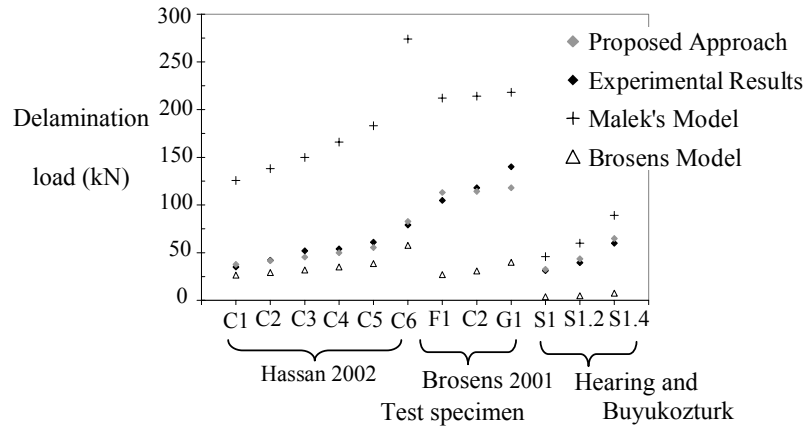


Figure 7. Experimental results compared with the proposed approach

## CONCLUSIONS

- (a) The efficiency of using CFRP bars as NSM reinforcement is controlled primarily by the bond characteristics of the bars as well as by the bond between the adhesive material and the concrete.
- (b) Two different types of interfacial debonding failures can occur for NSM FRP bars: i- Epoxy split failure ii- Concrete split failure.
- (c) Increasing the groove width and/or using high strength concrete, increases the resistance to concrete split failure. Using high strength adhesives and/or increasing the epoxy cover layer delays epoxy split failure for NSM FRP bars.
- (d) The proposed analytical models and failure criteria for NSM FRP strips as well as for externally bonded FRP sheets are capable of predicting the interfacial shear stress distribution, ultimate load carrying capacity and mode of failure.

## REFERENCES

1. Rizkalla, S., and Hassan T., "Effectiveness of FRP techniques for strengthening concrete bridges" *Journal of the International Association for Bridge and Structure Engineering*, 12(1), 2002.
2. Hassan, T., and Rizkalla, S., "Investigation of bond in concrete structures strengthened with near surface mounted CFRP strips." *ASCE, Journal of Composites for Construction*, 2002, *in press*.
3. Malek, A., Saadatmanesh, H., and Ehsani, M., "Prediction of failure load of R/C beams strengthened with FRP plate due to stress concentration at the plate end", *ACI Structural Journal*, 95(1), 1998, pp.142-152.
4. Hassan, T., "Flexural behavior and bond characteristics of FRP strengthening techniques for concrete structures", *Ph.D. Thesis*, University of Manitoba, Canada, 2002, 304 p.
5. Brosens, K., "Anchorage of externally bonded steel plates and CFRP laminates for the strengthening of concrete elements", *Ph.D. Thesis*, K. U. Leuven, Belg., 2001, 225 p.
6. Hearing, B. and Buyukozturk, O., "Delamination in reinforced concrete retrofitted with fibre reinforced plastics", *Ph.D. Thesis*, MIT, 2000, 287p.

